



Epigenetic and evolutionary features of ape subterminal heterochromatin

DongAhn Yoo, Katherine M. Munson and Evan E. Eichler

Genome Res. 2026 36: 38-49 originally published online October 22, 2025

Access the most recent version at doi:[10.1101/gr.280987.125](https://doi.org/10.1101/gr.280987.125)

References This article cites 36 articles, 7 of which can be accessed free at:
<http://genome.cshlp.org/content/36/1/38.full.html#ref-list-1>

Open Access Freely available online through the *Genome Research* Open Access option.

Creative Commons License This article, published in *Genome Research*, is available under a Creative Commons License (Attribution 4.0 International), as described at <http://creativecommons.org/licenses/by/4.0/>.

Email Alerting Service Receive free email alerts when new articles cite this article - sign up in the box at the top right corner of the article or [click here](#).

To subscribe to *Genome Research* go to:
<https://genome.cshlp.org/subscriptions>

Epigenetic and evolutionary features of ape subterminal heterochromatin

DongAhn Yoo,¹ Katherine M. Munson,¹ and Evan E. Eichler^{1,2}

¹Department of Genome Sciences, University of Washington School of Medicine, Seattle, Washington 98195, USA; ²Howard Hughes Medical Institute, University of Washington, Seattle, Washington 98195, USA

Many African great ape chromosomes possess large subterminal heterochromatic caps at their telomeres that are conspicuously absent from the human lineage. Leveraging the complete sequences of great ape genomes, we characterize the organization of subterminal caps and reconstruct the evolutionary history of these regions in chimpanzees and gorillas. Detailed analyses of the composition of the associated terminal 32 bp satellite array from chimpanzee (termed pCht) and intervening segmental duplication (SD) spacers confirm two independent origins in the *Pan* and gorilla lineages. In chimpanzee and bonobo, we estimate these structures emerged ~7.7 million years ago (MYA) in contrast to gorilla, in which they expanded more recently, ~5.0 MYA, and now make up 8.5% of the total gorilla genome. In both lineages, the SD spacers punctuating the pCht heterochromatic satellite arrays correspond to pockets of decreased methylation, although in gorilla such regions are significantly less methylated ($P < 2.2 \times 10^{-16}$) than in chimpanzee or bonobo. Allelic pairs of subterminal caps show a higher degree of sequence divergence than euchromatic sequences, with bonobo showing less divergent haplotypes and less differentially methylated spacers. In contrast, we identify virtually identical subterminal caps mapping to nonhomologous chromosomes within a species, suggesting ectopic recombination potentially mediated by SD spacers. We find that the transition regions from heterochromatic subterminal caps to euchromatin are enriched for structural variant insertions and lineage-specific duplicated genes. Our findings suggest independent evolution of subterminal caps converging on a common genetic and epigenetic structure that promoted ectopic exchange as well as the emergence of novel genes at transition regions between euchromatin and heterochromatin.

[Supplemental material is available for this article.]

With respect to humans, chromosome karyotypes of nonhuman African great apes (chimpanzee, bonobo, and gorilla) differ by the presence of subterminal heterochromatic caps, which were recognized cytogenetically >40 years ago (Yunis and Prakash 1982). Among chimpanzee, gorilla, and bonobo, the subterminal caps are differentially distributed among chromosomes. These caps are composed of hundreds of kilobase pairs of long satellite arrays in which the basic repeat unit, known as pCht satellite (also called as StSat or subterminal satellite), is 32 bp in length (Royle et al. 1994; Koga et al. 2011; Ventura et al. 2012). Previous cytogenetic studies in chimpanzees have shown that subterminal caps can form unique terminal associations in 32% of spermatocytes during late meiotic prophase I, the so-called postbouquet structures. These cytogenetic structures are thought to promote ectopic recombination through persistent interactions between subtelomeric sequences among homologous and nonhomologous chromosomes (Hirai et al. 2019). The function of the subterminal caps is not known, although they have been proposed to help stabilize African great ape genomes by preventing or buffering against interchromosomal exchanges of more proximal subtelomeric sequences (Hirai et al. 2019) or contributing to the replication biology of telomeres (Novo et al. 2013).

Subsequent investigations into the organization of these regions discovered segmental duplication (SD) “spacers” interdigitated between the large arrays of pCht satellite DNA (Ventura et al. 2012; Yoo et al. 2025). SD spacers of different phylogenetic

origin were identified in the *Pan* and gorilla lineages, suggesting that the subterminal cap structures arose independently. Previous studies proposed an evolutionary model in which a human–chimpanzee pericentric inversion followed by Chromosome 2 fusion contributed to the predisposition or loss of subterminal caps in nonhuman apes and human genomes (Royle et al. 1994; Ventura et al. 2012). Jiang and colleagues (2024) further refined the Chromosome 2 fusion breakpoint and subterminal SDs in humans. In the most recent study, the heterochromatic cap sequences were fully resolved using a hybrid long-read assembly approach (Oxford Nanopore Technologies [ONT] and Pacific Biosciences [PacBio] high-fidelity [HiFi]) and assembly phasing (HiC and parent–child trios) (Yoo et al. 2025).

Although these subterminal satellites are absent in other apes like orangutans (Haaf and Schmid 1987; Ijdo et al. 1991; Ventura et al. 2011), such structures are not unique to African great apes. A similar, albeit larger, subterminal heterochromatic cap structure composed of alpha-satellite DNA was described for siamang genomes from the gibbon lineage (Koga et al. 2012). We recently characterized the heterochromatic cap sequence and structure of the siamang genome (Yoo et al. 2025). Although it is similar in form to that of the great apes (i.e., blocks of satellite interdigitated with a spacer that shows epigenetically reduced methylation), the component sequences completely differ. In siamang, there is no pCht satellite but instead alpha-satellite sequence, and the spacer is made up of a 50 kbp SD of different origin than either the *Pan* or gorilla spacer. The independent emergence of subterminal satellite structures in multiple primate lineages (gorilla, chimpanzee, and

Corresponding author: ee3@uw.edu

Article published online before print. Article, supplemental material, and publication date are at <https://www.genome.org/cgi/doi/10.1101/gr.280987.125>. Freely available online through the *Genome Research* Open Access option.

© 2026 Yoo et al. This article, published in *Genome Research*, is available under a Creative Commons License (Attribution 4.0 International), as described at <http://creativecommons.org/licenses/by/4.0/>.

siamang) so similar in structure and epigenetic form suggests convergent evolution of potential functional significance. In this study, we leverage the fully resolved sequence of telomere-to-telomere (T2T) ape genomes to more systematically investigate the evolution, structure, and epigenetic properties. The availability of two fully resolved haplotype assemblies from each ape species allowed for investigations into patterns of allelic variation and between-species comparisons of subterminal organization and differences in methylation patterns. We examined the telomeric transition regions from heterochromatin to euchromatin, leading to potentially new insights into the genic content and stability of these regions across ape genomes.

Results

African great ape subterminal heterochromatin cap structure and methylation

Using the recently published ape T2T genomes (Supplemental Table S1; Yoo et al. 2025), we estimated the size and content of

each chromosomal cap in chimpanzee, bonobo, and gorilla (Fig. 1; Supplemental Table S2), defining chromosomes based on their synteny with human (McConkey 2004). Overall, gorilla chromosomes have a larger and greater number of subterminal caps in which they account for 584.1 Mbp (8.46%) of the diploid genome, whereas those of chimpanzee and bonobo genomes represent 337.9 and 314.7 Mbp (5.4% and 5.0%), respectively. We identified subterminal caps on both homologs (allelic pairs) in both chimpanzee and gorilla, whereas bonobo showed patterns consistent with heteromorphic variation (present on only one of two homologous chromosomes). For example, the bonobo p-arms of Chr14 (hsa13) and Chr19 (hsa17) and both p- and q-arms of Chr18 (hsa16) possessed subterminal caps on only one of the two haplotypes for this individual. This heteromorphism and the fact that bonobo possesses the lowest number of subterminal caps ($n=46$ compared with 57 in chimpanzee and 79 in gorilla) suggest that the caps are less prominent or less stable in this species, although we caution that additional samples need to be examined. Notably, the short (p-) arms of chimpanzee and bonobo more consistently harbor a greater number of subterminal caps (39 and 31) compared

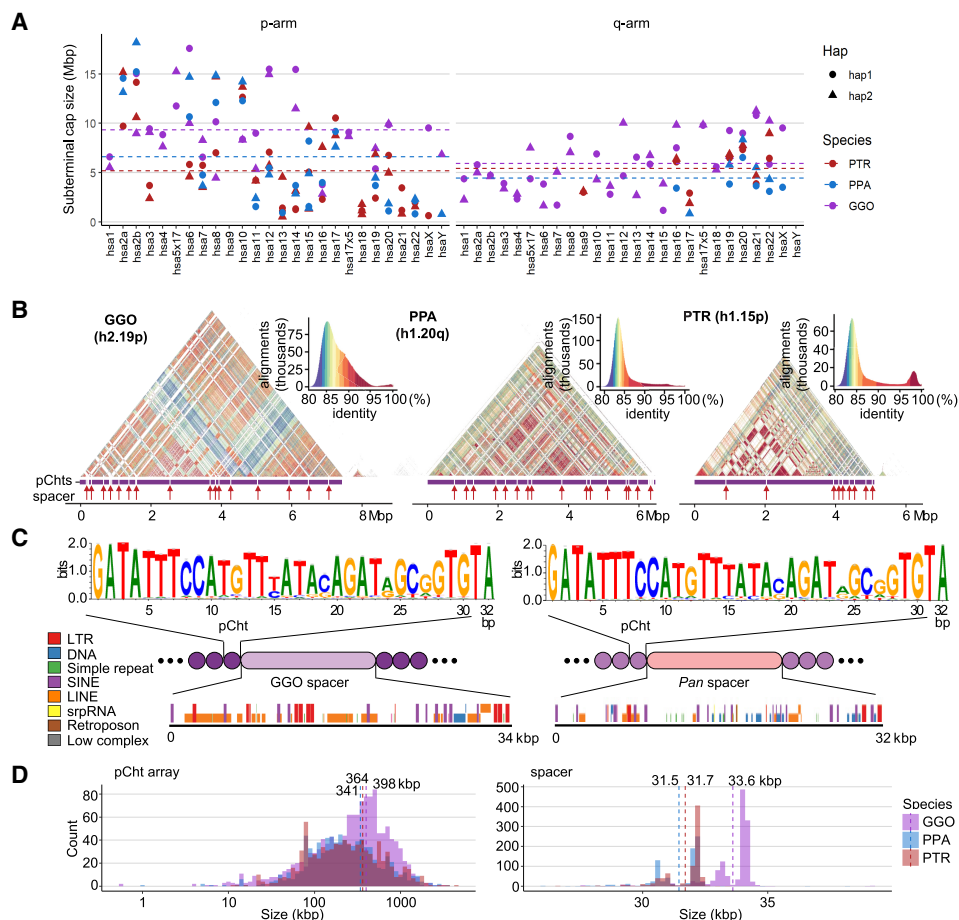


Figure 1. Overview of African great ape subterminal cap organization. (A) Size of p- or q-arm subterminal caps in three species: chimpanzee (PTR), bonobo (PPA), and gorilla (GGO), indicated by red, blue, and purple, respectively. Circles and triangles indicate haplotypes 1 and 2, or maternal and paternal for bonobo and gorilla, respectively. (B) StainedGlass (Vollger et al. 2022) self-alignment plot of subterminal caps including pCht satellites indicated by the purple track below the triangular heatmap, as well as subterminal SD spacers interrupting satellite arrays, indicated by the red arrows below. (C) The structure of subterminal caps. From the top, the logo base profile of pCht satellite is shown, followed by the higher-order structure of subterminal cap sequences, and the sequence composition of the subterminal SDs at the bottom. (D) Size distribution of uninterrupted pCht array and subterminal SDs. The dotted line indicates the mean. The x-axis is in a \log_{10} scale for the pCht array owing to variation in its size.

with q-arms (14 and 11). In contrast, the gorilla genome shows a more uniform distribution with more q-arm (45) subterminal caps than p-arms (34). The lengths of the subterminal caps were highly variable, ranging from <1 Mbp in chimpanzee Chr14 (hsa13) to a 35-fold longer length of 18.9 Mbp in bonobo Chr6 (hsa7) (Fig. 1A). Unlike gorilla, two interstitial satellite arrays are observed in chimpanzee and bonobo mapping to Chr6 (hsa7) and 14 (hsa13) (Royle et al. 1994).

As previously reported (Yoo et al. 2025), analysis of the subterminal caps revealed a higher-order organization of pCht satellite arrays of variable length (ranging from <10 kbp to hundreds of kilobase pairs with a mean of 341–398 kbp) interdigitated with SD spacers (Fig. 1B–D; Supplemental Fig. S1). We find that pCht satellites are generally >80% identical with the ones in closer proximity showing higher identity within a chromosomal arm (Fig. 1B). Although different subtypes of pCht can be distinguished, we derived a consensus for each depending on species (Fig. 1C; Supplemental Fig. S2). Despite the sequence variation, we find that the gorilla satellite consensus is almost identical to that of the *Pan* lineage (chimpanzee and bonobo), with the exception of the thymine in the 15th position, which shows less variability in the *Pan* lineage. In terms of epigenetic status, we investigated methylation patterns of both spacers and satellites. Although we have data from both PacBio and ONT, we chose to focus on methylation calls from ONT for two reasons. First, previous studies (Liu et al. 2022; Sigurpalsdottir et al. 2024) have shown greater sensitivity in detection, and second, ultralong reads are necessary to uniquely anchor reads in long stretches of DNA. Our study finds these satellite sequences show high levels of 5mC methylation, with gorilla showing average methylation of 83.3% compared with 78.4% in bonobo and 73.6% in chimpanzee (Supplemental Figs. S3, S4A).

The pCht satellite arrays are interrupted irregularly by pockets of less methylated subterminal SD spacers (Supplemental Figs. S3, S4). These SDs originate from euchromatic sequence in the ancestral ape lineage (Fig. 1C). For example, the ancestral subterminal SD spacer in gorilla maps to the intronic region of the gene *MALDI* of Chr8 (hsa10, p12.31) and subsequently expanded to about 700 copies per gorilla haplotype. In contrast, the spacer of the *Pan* lineage originates from a subsequence of *PGM5*, Chr11 (hsa9, q21.11) (Supplemental Fig. S5), and expanded to about 413 and about 430 copies per haplotype for chimpanzee and bonobo, respectively (Supplemental Table S3). The gorilla spacers contained 1.8-fold greater LINE content and *Pan* spacers 2.4-fold greater DNA transposon content compared with euchromatic regions; however, we found no statistical significance from this comparison (one-sided permutation test $P=0.15$ and 0.07 , respectively). The average length of the gorilla and *Pan* spacers are 34 and 32 kbp, respectively (Fig. 1C,D). Of note, the length of both spacers and pCht arrays is significantly longer in gorilla compared with chimpanzee and bonobo (two-sided Wilcoxon test $P < 2.2 \times 10^{-16}$ and $P = 6 \times 10^{-10}$, respectively) consistent with their independent origin and expansion in each lineage (Ventura et al. 2012).

Examining the epigenetic status of SD spacers, we find a significantly lower rate of 5mC methylation in gorilla (average of 38.8%) relative to chimpanzee (40.2%) and bonobo (49.9%), with $P < 2.2 \times 10^{-16}$, two-sided Wilcoxon test (Supplemental Figs. S3, S4B). Using SD spacers mapping outside of pCht satellite arrays as a comparative control, we find that 99.8% and 98.5% of gorilla and chimpanzee spacers are less methylated, whereas only 17.8% of bonobo spacers are less methylated than their interstitial paral-

ogs (Supplemental Fig. S4B). In chimpanzee and bonobo, spacer length positively correlates with CpG methylation, although no such pattern is observed for gorilla, in which reduced methylation of spacer is much more uniform (Supplemental Fig. S4C). Using previously generated Iso-Seq data (Makova et al. 2024; Yoo et al. 2025), we were unable to identify spliced transcripts originating from the pCht satellite arrays or SD spacers (Supplemental Tables S4, S5), although we note that Iso-Seq has relatively low sensitivity of detection (Novo et al. 2013).

Evolution of the spacer and satellite sequence

To reconstruct the evolutionary history of the subterminal satellites, we performed an independent analysis of the two classes of repeats that define its composition: the pCht (~32 bp) satellite that exists in millions of copies throughout the ape genomes and the *Pan* and gorilla SD spacers (32–34 kbp) that represent independent SD expansions (400–700 copies per genome) in association with the pCht satellites. Although the SD spacer is far less abundant than the pChts, its length is thousands of times longer, providing a robust signal for multiple sequence alignment (MSA), phylogenetic reconstruction, and timing estimates.

For the pCht satellites, we first extracted all pCht units from the chimpanzee ($n=6,881,426$), bonobo ($n=6,616,396$), and gorilla ($n=14,248,529$) subterminal caps. From this, we selected the most abundant 19,012 pCht variants (85% of the total pChts) that occur more than 100 times in these genomes. Under the assumption that more closely related subterminal arms would likely share a similar pCht composition, we performed an all-to-all pairwise comparison between subterminal heterochromatic caps that contain at least 2000 pChts to identify those that are more closely related to one another. We applied unsupervised hierarchical clustering (pvclust) (Suzuki and Shimodaira 2006) across the three species and constructed a tree based on normalized counts of each pCht variant between subterminal heterochromatic caps (Methods) (Fig. 2A). The composition of pCht variant types clearly distinguishes the gorilla and *Pan* lineages with the exception of the Chr5 (hsa6) q-arms of gorilla, which groups with the subterminal caps (ChrX) from the *Pan* lineage (Fig. 2A). This suggests a possible common origin, but the majority of the subterminal caps have formed independently as a result of recurrent expansions in each lineage. Among the subterminal caps from chimpanzee and bonobo, pCht variant compositions do not distinguish between the two species. The similarity in composition may arise from the pCht sequences sharing a common origin or subsequent gene flow between the two lineages after speciation (Fontseré et al. 2022).

Intraspecies sequence comparisons of the subterminal satellites show that some nonhomologous chromosomes are more similar in composition than their allelic counterparts; that is, homologous subterminal caps do not always pair (e.g., GGO.h2.3p vs. GGO.h1.Xp) (Fig. 2A). Under the assumption that nonhomologous subterminal caps are subject to ectopic recombination (Ventura et al. 2012; Hirai et al. 2019), we sought to classify the major pCht subtypes using a two-step *k*-means clustering approach (Methods) (Supplemental Fig. S6). We identified eight higher-order satellite block types across the 167 subterminal caps (Fig. 2B) from the three ape species. Consistent with the hierarchical clustering tree, the gorilla and *Pan* lineages are largely distinct. Gorilla subterminal caps consist of k2, k4, and k5 block types, whereas the *Pan* lineage caps are composed of k3, k6, k7, and k8 types. Once again, gorilla Chromosome 5 (hsa6) is an

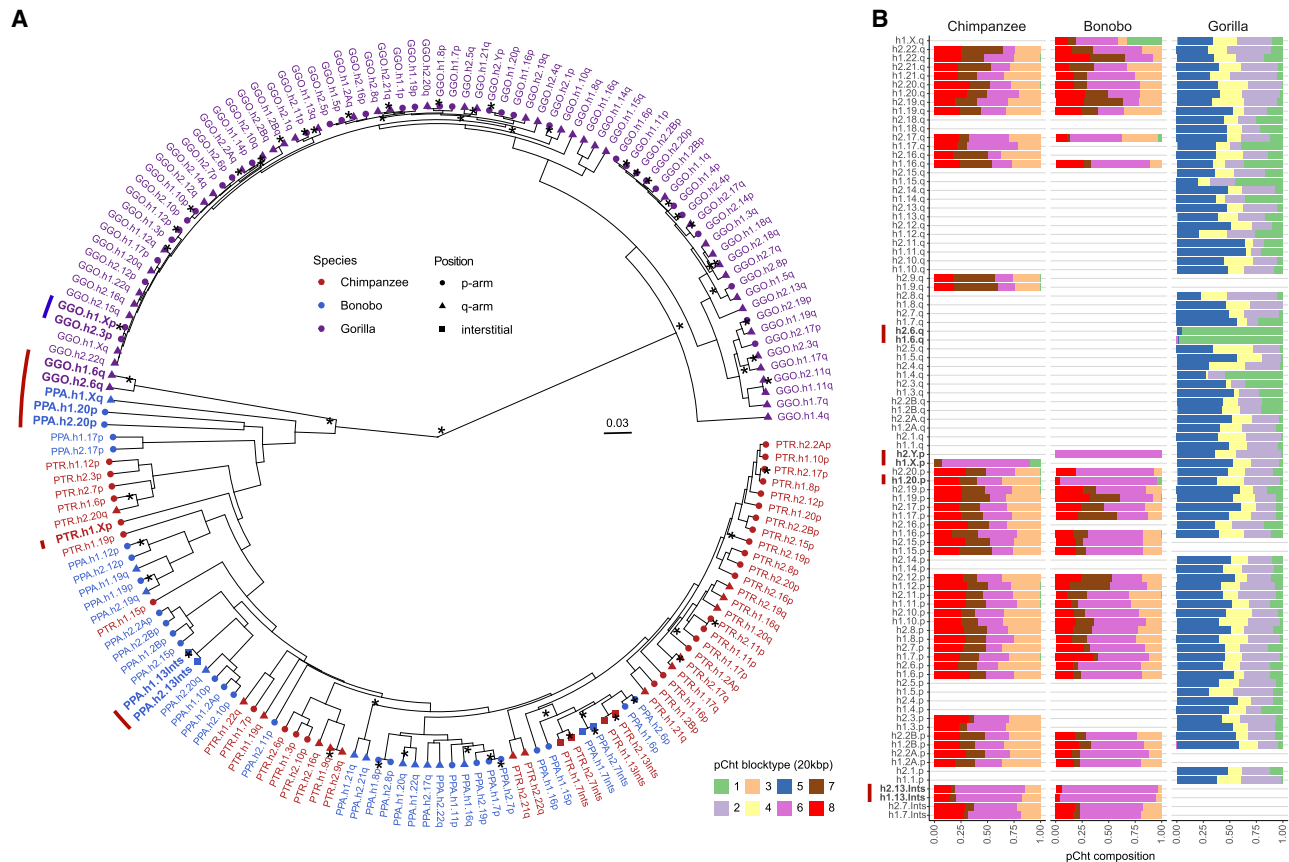


Figure 2. pCht satellite higher-order structure and phylogeny. (A) Clustering of the subterminal arms based on relative abundance of pCht variants. Each terminal node indicates species (chimpanzee, PTR; bonobo, PPA; and gorilla, GGO), human chromosome number, and whether the position of the subterminal cap is located in p-arms, q-arms, or interstitial (Ints). The top 5% of subterminal caps with the largest proportion of shared pCht types (among GGO and *Pan*) are highlighted (bold/red line) (Supplemental Fig. S7C). GGO.h2.3p versus GGO.h1.Xp (blue line) is an example in which the nonallelic subterminal cap pair is more closely related than the allelic pair. Internal nodes with a bootstrap score higher than 95 are indicated by a star. (B) Identification of eight higher-order block types (20 kbp) of pCht satellites across the subterminal caps of three African great apes. The highest proportion of shared pCht types among chimpanzees and gorillas are indicated (red line).

exception with a largely uniform composition of the k1 block type, which is shared with the X Chromosome p-arms of bonobo and chimpanzee and to a lesser degree with a fraction of other *Pan* autosomes. The k1 block type, thus, is distinct in being the only block type shared among the gorilla and *Pan* lineages, potentially identifying the ancestral pCht. We also note that this block type is composed of the largest portions of common pChts shared among *Pan* and gorilla (Supplemental Fig. S7).

As a second approach, we used the SD spacer sequences of the gorilla and *Pan* lineages as a proxy to trace the evolutionary history of the subterminal heterochromatic caps. In this approach, we extracted a shared segment (>20 kbp in length and >90% identity) from the spacer for gorilla and the spacer for the *Pan* lineage and generated an MSA to construct a maximum likelihood phylogenetic tree for each lineage (Methods) (Fig. 3). Using Asian apes as an outgroup (Methods), the gorilla spacer phylogenetic tree predicts that the ape ancestral locus (hsa10) began to duplicate 5.6 (5.1–6.1) million years ago (MYA), creating an interstitial copy mapping to *Pan* Chr6 (hsa7) that is located 2 kbp away from an interstitial pCht satellite array. This interstitial spacer in the *Pan* lineage is ancestral to all other gorilla subterminal cap spacers beginning to duplicate soon thereafter (5.0 [4.5–5.6] MYA) (Fig. 3A), although it is no longer identified at the syntenic location in gorilla or hu-

man. The topology of the gorilla phylogenetic tree suggests a series of initial stepwise duplications; for example, the gorilla Chr5 (hsa6) q-arm is estimated to have occurred 3.8 (3.4–4.4) MYA. After these initial duplications, a subsequent burst of gorilla spacers began to occur 2.5 (2.1–2.9) MYA, giving rise to the majority of SD spacers in the gorilla genome. We also note that the phylogenetic tree of the duplicated spacers shows signs of incomplete lineage sorting (ILS), which does not follow the species tree (Fig. 3), consistent with additional trees (Supplemental Fig. S8).

Although the SD spacer in the *Pan* lineage differs with respect to its ancestral origin (hsa9), similar to gorilla it is predicted to begin its duplication in the common ancestor of humans, chimpanzees, and gorillas, creating multiple interstitial copies (hsa4, 5, 8, and X) as well as copies located subterminal of hsa2A/2B, the fusion point (Jiang et al. 2024) for the formation of human Chromosome 2 (Fig. 3B). Overall, the branch lengths or sequence identity of the chimpanzee phylogeny are significantly longer ($P < 2.2 \times 10^{-16}$ by two-sided Wilcoxon test) (Supplemental Fig. S9) than that of gorilla, consistent with a series of more ancient duplications in the *Pan* lineage. We estimate the oldest divergence time among the *Pan* lineage SD spacers to be 7.7 (7.2–8.5) MYA, which is close to the divergence time of human and gorilla ancestral orthologs (8.6 [8.3–9.3] MYA) (Kumar et al. 2022). The chimpanzee SD

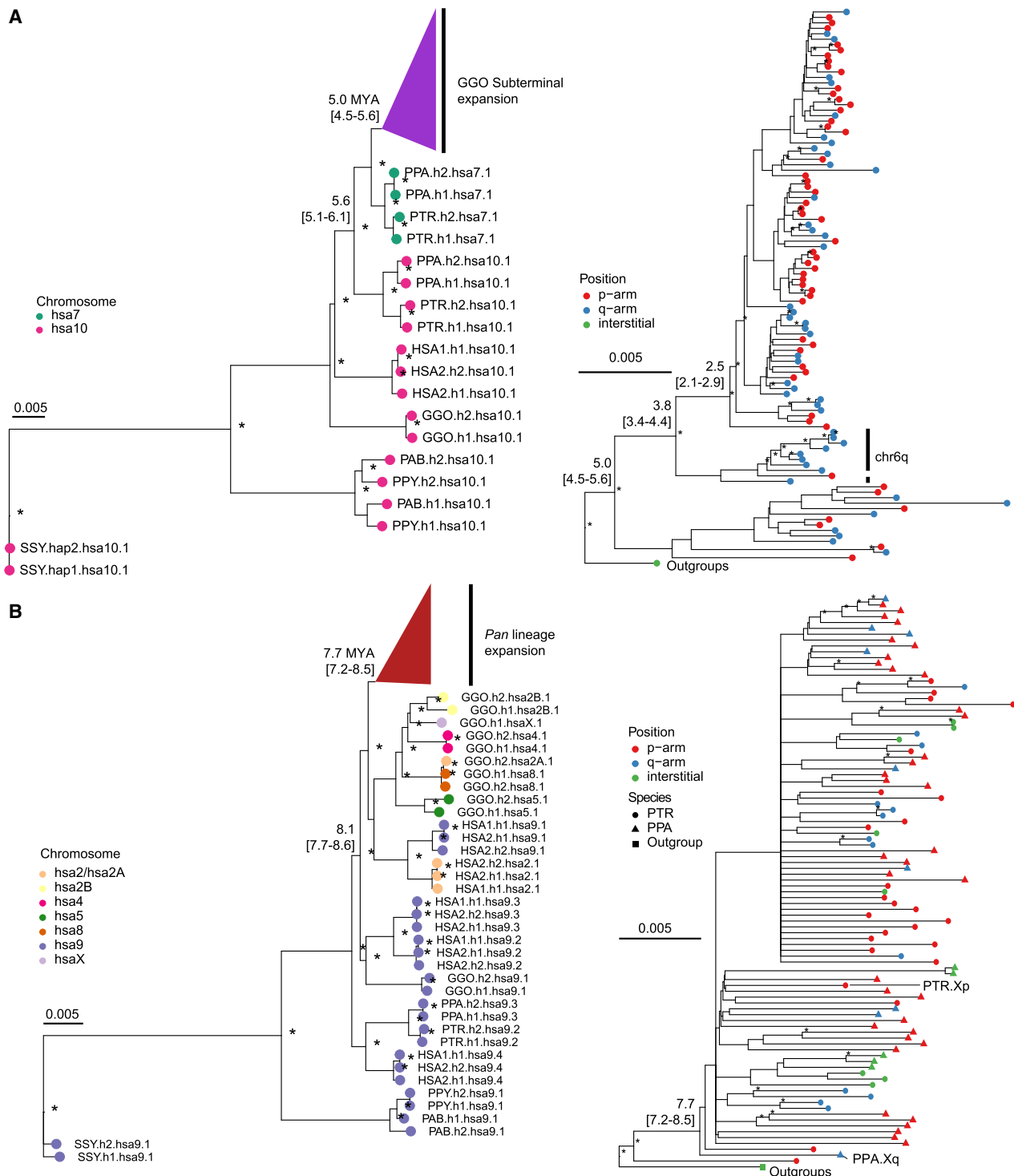


Figure 3. Evolution of subterminal SD spacers. (A,B) Maximum likelihood phylogenetic tree of gorilla (34 kbp; A) and *Pan* subterminal SDs (32 kbp; B) constructed from total spacers (showing subset of $n = 100$ copies). In each, the *left* panel shows the overall topology with a time-scale tree calibrated to orthologous ancestral primate copies. Chromosome numbers (based on human chromosome synteny) are color-coded and labeled by haplotype (h1 or h2) and species acronym: human (HSA; HSA1-CHM13, and HSA2-HG002), chimpanzee (PTR), bonobo (PPA), gorilla (GGO), Sumatran orangutan (PAB), Bornean orangutan (PPY), and siamang (SSY). A colored triangle denotes the subterminal spacer expansion. The *right* panel zooms into the subterminal spacer topology and time estimates in million years ago (MYA) with 95% confidence interval in the bracket. Gorilla (*top*) and chimpanzee (*bottom*) spacers are classified as p-arm (red), q-arm (blue), or interstitial (green). In addition, for the *bottom* panel, species are indicated as outgroup (rectangle), chimpanzee (circle), or bonobo (triangle) in origin. Internal nodes with bootstrap score higher than 95 are indicated by a star.

spacers associated with the ChrX p-arm subterminal caps, which also share ancient higher-order pCht blocks, represent some of the most ancient spacer duplications (Fig. 3B). Similar to gorilla, the topology of the chimpanzee spacer tree predicts a burst of duplications, albeit much older (average of terminal branch length, 1.3 MYA) compared with that of gorilla (average of 0.4 MYA) (Supplemental Fig. S9B). It should be noted, however, that the spacers from homologous chromosome arms do not always cluster, potentially as a result of ectopic recombination.

Patterns of allelic and nonallelic variation

A striking feature of the subterminal heterochromatic caps is the high degree of allelic sequence diversity observed between two haplotypes (Fig. 4A–C; Supplemental Data). Only 12% (10/82) of haplotype comparisons show >99% sequence identity with >50% alignment coverage. Most haplotype comparisons show >10% sequence divergence (Supplemental Figs. S10–S13). A comparison with other genomic regions, including centromere, acrocentric, and remaining regions, reveals that subterminal caps were the regions with the greatest degree of allelic divergence (Supplemental Fig. S14). Notably, the degree of allelic divergence differs among the species. Gorilla and chimpanzee show, on average, greater sequence divergence (10.8% and 11%, respectively) compared with bonobo (8.7%) (Fig. 4D). When comparing nonallelic versus allelic sequence identity, gorilla and chimpanzee distributions are largely indistinguishable, in contrast to bonobo, in which allelic alignments now show significantly greater allelic sequence identity compared with nonallelic alignments (Fig. 4E). This feature is reflected in a matrix percentage identity plot in which each subterminal haplotype is aligned to every other within the individual (Fig. 4B,C). Compared to bonobo, in which more than a one-third of the allelic comparisons show the highest degree of sequence identity (as indicated by the diagonal in Fig. 4C), gorilla shows no such pattern. Instead, allelic and nonallelic patterns are largely indistinguishable, perhaps providing evidence of more rapid, ongoing ectopic recombination occurring in this lineage.

As part of our all-by-all alignment analysis of subterminal caps, we searched for specific examples in which there was evidence of a recent ectopic exchange (>99.5% identity) between nonhomologous chromosomes. We identified 11 candidates for ectopic exchange (eight in gorilla, three in chimpanzee, and none in bonobo). For example, we identified a potential 5 Mbp ectopic exchange between GGO.3p (Chr2/hsa3) and Chromosome Xp (Fig. 5A). We refined the breakpoints of the sequence exchange and mapped both to different SD-spacer regions, corresponding to the third and 25th SD spacer positions on the short arm of the gorilla X Chromosome (Fig. 5B). Analyzing the remaining candidates (Fig. 5C; Supplemental Figs. S15–S17), we found three out of eight examples in which the breakpoint mapped precisely within the spacer and two additional examples in which one of the breakpoints mapped within 10 kbp of a spacer. Given that the SD spacers represent a small fraction of the subterminal heterochromatic cap, we performed a simulation to test the proximity of breakpoints to SD spaces. We find that candidate breakpoints of recent ectopic exchange (>99.8 identity) are more likely ($P=0.035$, one-sided Wilcoxon ranked-sum test) (Supplemental Fig. S18) to map in close proximity to SD spacers than expected based on a null subterminal distribution (Fig. 5D).

As a final test of the potential role of SD spacers in mediating ectopic exchange, we developed a phylogenetic approach to test for this association. We reasoned that if spacers were preferential

sites of ectopic recombination during evolution, dividing the ~30 kbp spacer sequence into two segments (first and second half, located at telomere and centromere directions, respectively) would capture two distinct phylogenetic histories when comparing them to each other (Supplemental Fig. S19) or to the topology of the full SD spacer (Fig. 5E). To test for significance, we calculated the distribution of Robinson–Foulds metric between individual bootstrap tree topologies (each replicate with $n=1000$) to their consensus topology to generate a null distribution of the expected statistic and contrasted this with the partial sequence trees (Fig. 5F). We find a significant shift in the topology of the SD spacer subset trees ($P<0.001$) for all three species (gorilla, chimpanzee, and bonobo), suggesting that historically the SD spacers may have been the preferential point of ectopic exchange between nonhomologous chromosome arms.

Subterminal heterochromatic–euchromatic transition regions and the evolution of new genes

Finally, we examined the euchromatin boundaries and putative evolutionary consequences and epigenetic features of the subterminal caps (Fig. 6). Specifically, we compared ape species with (gorilla/chimpanzee) and without (Bornean and Sumatran orangutans) subterminal caps to determine if the rate of structural variation, gene density, and methylation differ in association with the evolution of these large terminal heterochromatic structures (Yoo et al. 2025). Using the human genome as a reference, we find ~24–72 Mbp of novel insertions mapping within 2 Mbp from the subterminal caps (African nonhuman apes) or telomeres (Asian great apes without subterminal caps) (Fig. 6A,B). The insertions in the African apes are notably more abundant (31.8–72.2 Mbp vs. 23.8–23.9 Mbp in orangutans) and larger (>10–500 kbp in size) compared with the Asian great apes (Fig. 6C; Supplemental Fig. S27). This is despite the fact that divergence time between humans and African great apes is close to half the divergence to Asian great apes. We estimate that 36%–42% of the inserted sequences in African apes originated from nonhomologous chromosomes (Supplemental Fig. S28), a potential consequence of the ectopic exchanges extending beyond the subterminal heterochromatic cap.

Leveraging CpG methylation signals associated with the long-read sequence data used to generate these ape assemblies (Yoo et al. 2025), we investigated methylation at the euchromatin–heterochromatin boundary defined here as the last proximal subterminal pCht satellite unit. Within 200 kbp of this transition, we observe an immediate and sharp drop (~54%) in methylation among nonhuman African great apes (Fig. 6D; Supplemental Fig. S29; for Asian great apes, see Supplemental Fig. S30), which quickly resets to a moderate level of hypermethylation (71%) when extended further euchromatically. Correlating with the transition to the lower methylation, we also observe the highest density of SDs and species-specific annotated duplicated genes (Yoo et al. 2025), which also reduces when extended more proximally into the euchromatin of gorilla (Fig. 6E) and chimpanzee (Supplemental Fig. S31). In Asian great apes, the signature of SDs and duplicated genes is less variable (Fig. 6E; Supplemental Fig. S31).

In total, we identify 204 novel duplicated genes at these subterminal euchromatin boundaries in gorilla ($n=85$), chimpanzee ($n=57$), and bonobo ($n=62$) (Fig. 6F; Supplemental Tables S6, S7). The enrichment of lineage-specific duplicated genes at this heterochromatin–euchromatin boundary is most extreme for gorilla (14.6-fold difference) followed by relatively high levels in

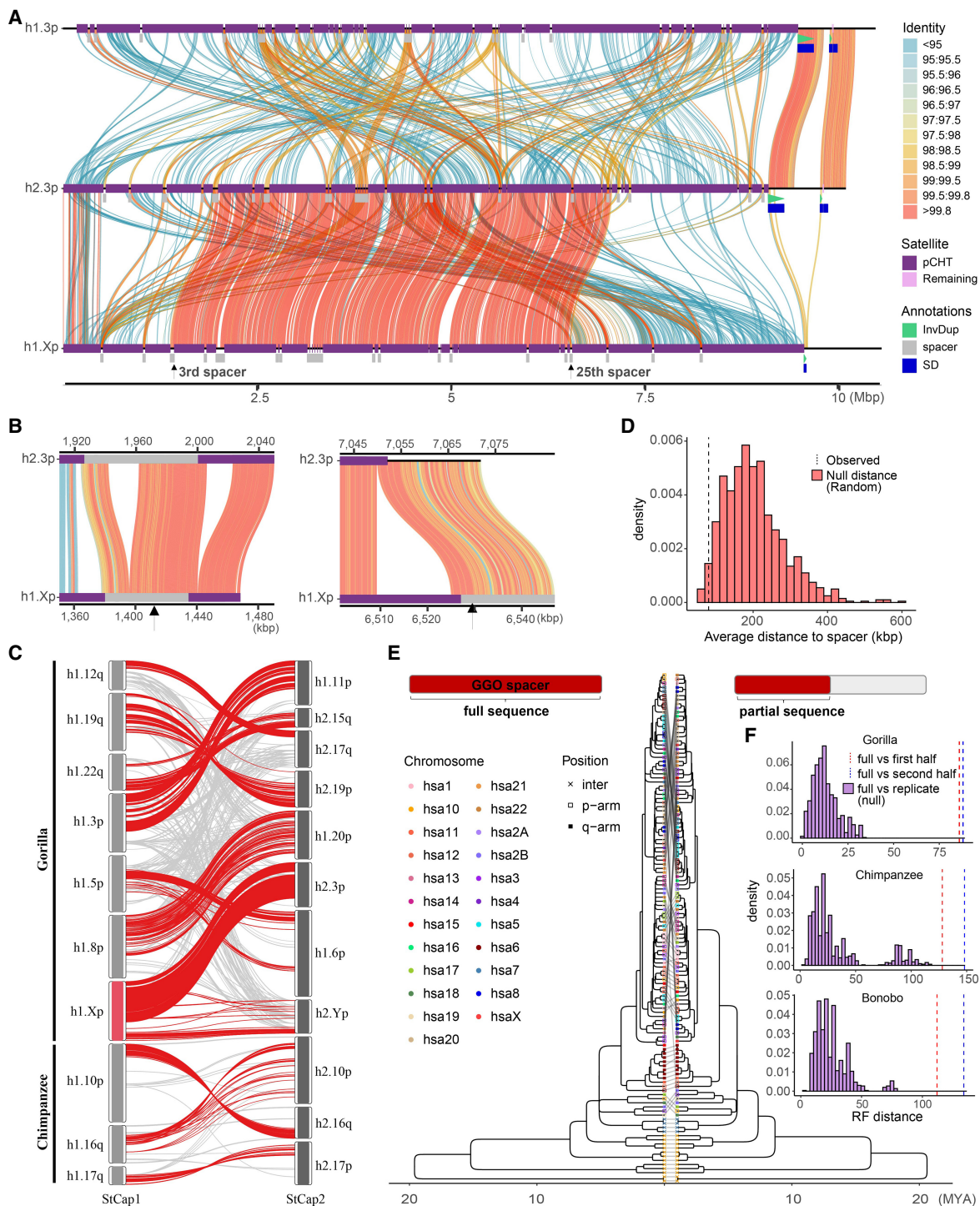


Figure 5. Evidence of nonallelic sequence exchange at SD spacers. (A) An alignment view (SVbyEye) (Porubsky et al. 2024) depicting a candidate ectopic exchange between subterminal satellite chromosomes hsa3 and hsaX p-arms of gorilla. The percentage identity of alignment (scaled from blue <95% to red >99.8%) with annotation tracks for higher-order pChT blocks, satellites, and SDs is shown on the right. (B) Enlarged view of the two exchange breakpoints (black arrows) mapping within the third and 25th SD spacers. (C) Overview of potential ectopic exchange events between the subterminal caps (left-StCap1 vs. right-StCap2 tracks) identified in African great ape genomes (eight and three events in gorilla and chimpanzee, respectively, including hsa3p vs. hsaXp in red). Assembly quality at the breakpoints was validated by a read-depth analysis in Supplemental Figures S20–S26. (D) Simulation test of exchange event breakpoints, suggesting that the exchange breaks (>99.8% identity alignment blocks; dotted line) are more likely to be located within or close to subterminal SD spacers compared with a random distribution (red histogram). (E, F) Comparison of maximum likelihood phylogeny to test recombination of SD spacer. A phylogenetic tree of the complete spacer sequence (left) is compared with that of a subset of the sequence (right). The tip nodes of the left tree are linked to the corresponding nodes of the right tree to visualize phylogenetic shifts in the topology. Robinson–Foulds (RF) distance is used to measure the extent of phylogenetic shift (first or last half sequences, in red and blue dotted lines, compared to a null distribution generated by computing distances of consensus tree vs. bootstrap replicate trees).

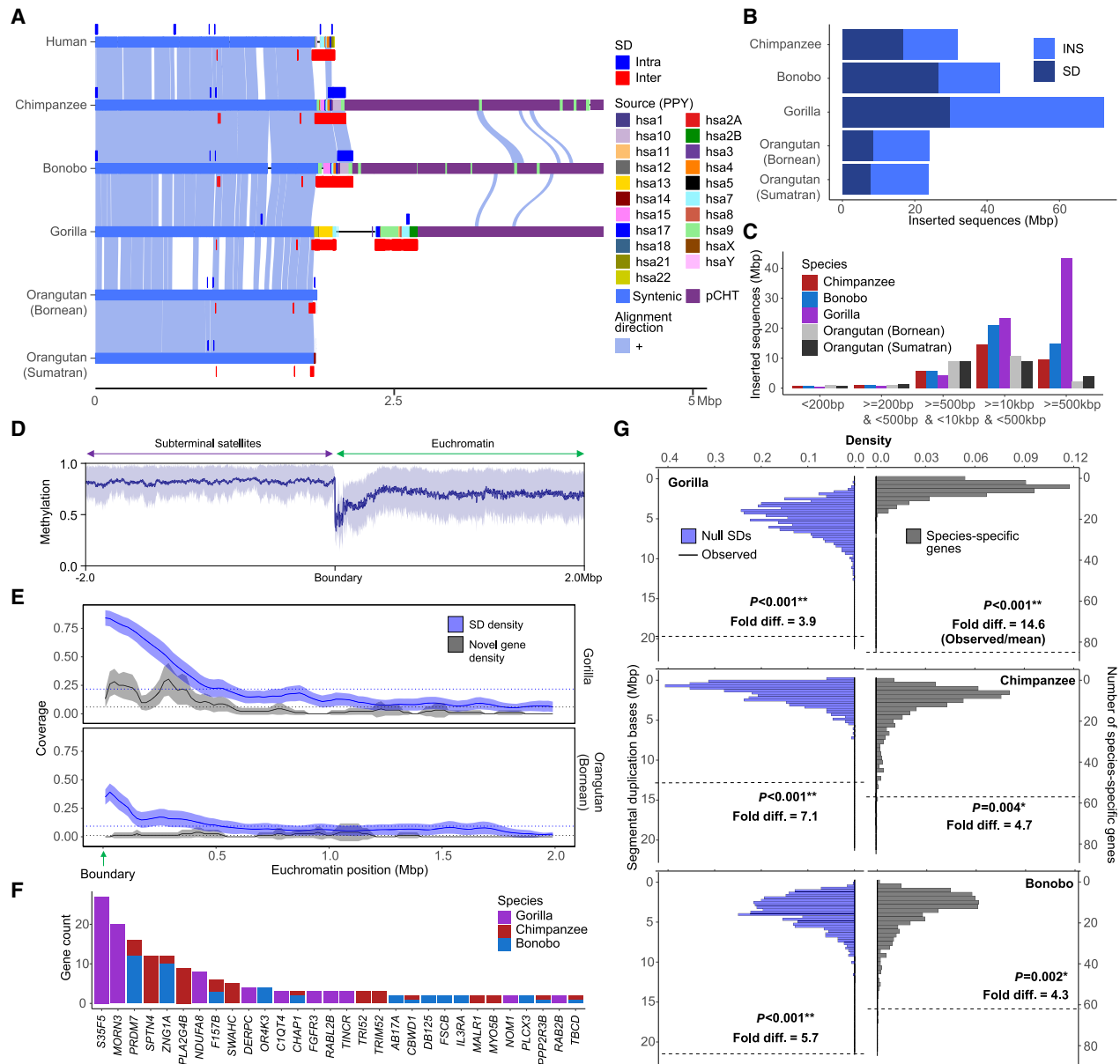


Figure 6. Duplicated genes and epigenetic features of ape genomes with and without subterminal caps. (A) An ape comparative analysis of the organization of subterminal sequences for the long arm of Chromosome hsa16. The stacked alignment plot (SVbyEye) contrasts syntenic euchromatic regions (light blue) with heterochromatic subterminal satellite regions (purple) and with the location of intra (dark blue) and interchromosomal (red) SDs along with the origin of the duplicated sequences (human chromosome designation). (B) The total number of new sequences (insertion [INS] or SD), not present in humans, at subterminal boundaries within 2 Mbp of the euchromatic–heterochromatic transition zone. (C) Size distribution of the total inserted sequences with respect to human genome, color-coded by species. (D) CpG methylation profile within 2 Mbp of the euchromatin–heterochromatin transition for chromosomes with subterminal caps in gorilla. The average percentage of CpG methylation (blue line) with standard deviation (blue shaded area) is shown. (E) The densities of SDs and novel genes at the euchromatic boundaries, highly enriched in gorilla, with subterminal caps, as opposed to the orangutan. The transparent area indicates 95% interval of the observed density. Dotted horizontal line indicates the mean density. (F) Duplicated genes and their copy number located at the boundary of subterminal caps, including eight genes validated by read depth of 120 primates (Mao et al. 2024). (G) Simulations to test enrichment of novel genes (Yoo et al. 2025) and SDs at the boundary of subterminal caps (2 Mbp) in gray and blue, respectively. The p indicates empirical P -value of the one-sided permutation test.

and we hypothesize that k1 was lost to the human lineage as a result of ILS or the Chromosome 2 fusion (Royle et al. 1994; Jiang et al. 2024). Second, subsequent hyperexpansion of pChT in the gorilla and *Pan* lineages created lineage-specific higher-order block types that now account for the bulk of the subterminal heterochromatic caps of each species. Third, using the SD spacer sequences as

a phylogenetic marker also supports early duplication and ILS. However, the phylogenetic analysis distinguishes two very different evolutionary trajectories. In the *Pan* lineage, both the formation and expansion (~7.7 [7.2–8.5] MYA) of the subterminal heterochromatin are much more ancient, far predating those of the gorilla SDs and the speciation of bonobo and the common

chimpanzee. In contrast, gorilla subterminal heterochromatin began to emerge 5.0 (4.5–5.6) MYA and hyperexpanded millions of years later (2.5–3.8 MYA). We predict the shared higher-order blocks (k1) of subterminal satellites identified in this study (Fig. 2B), as well as multicopy orthologs of *Pan* lineage SDs in gorilla and human are the remnants of the ancient African great ape subterminal heterochromatin in these genomes.

Although the general organization of the subterminal heterochromatic caps is similar among the nonhuman African apes, we document important epigenetic and genetic differences within each species. Owing to its more recent origin, gorilla subterminal heterochromatic caps are more homogenous among the nonhomologous chromosomes, and gorilla SD spacers show the most extensive reduction in CpG methylation. In contrast, bonobo subterminal heterochromatic caps are composed of the oldest or most divergent subterminal SDs and showed a higher degree of heteromorphism (present on only one of the two allelic homologs) compared with the other apes analyzed in this study, although this observation is based on only one individual per species. Combined with a demonstrable weaker methylation change for the SD spacers (Supplemental Fig. S4), much higher allelic identity (Fig. 4), and the fact that we find no evidence of recent ectopic sequence exchange in bonobo genomes, this again distinguishes the bonobo lineage, although we caution that additional bonobo genomes derived from primary tissues as opposed to cell lines will need to be assayed to establish this as a species-specific property. Although this may indicate a slower expansion or increased rate of decay, it may also be the result of some species-specific differences in repair or transfer of material between chromosomal homologs. Nevertheless, under this model, gorilla would be predicted to be the most active subterminal heterochromatic cap, perhaps explaining why it is much more prevalent in this genome adding almost three chromosomes worth of DNA (584 Mbp).

Since the first characterization of African great ape subterminal satellites, there has been limited investigation into the functional significance of subterminal heterochromatic caps. Based on FISH experiments in chimpanzee meiotic sperm cells in a previous study, Hirai et al. (2019) suggested that the subterminal heterochromatin was driving ectopic recombination by helping to form bouquet structures among nonhomologous chromosomes during late meiotic prophase, somewhat akin to the nuclear organizing structures associated with the repeat-rich short arms of mammalian acrocentric chromosome (Nurk et al. 2022). Hirai and colleagues (2019) further concluded that such subterminal associations may be selectively beneficial by providing greater stability or buffering capacity to subterminal regions of ape chromosomes, areas known to be genetically and evolutionarily unstable (Knight and Flint 2000; Mefford and Trask 2002). In our study, we provide further support for their involvement in ectopic recombination by identifying 11 potential examples of interchromosomal translocations (eight in gorilla and three in the common chimpanzee) (Fig. 5C). Both our breakpoint analysis of these events and our phylogenetic analysis indicate that the SD spacer regions are preferential drivers of this ectopic recombination between nonhomologous chromosome arms. It is possible that both the high degree of sequence identity of these 30 kbp segments and their reduced methylation status provide an ideal open-chromatin substrate for nonallelic homologous recombination, although the mechanism still remains to be determined. However, unlike Hirai et al.'s prediction of conferring genomic stability, our evolutionary analysis suggests the complete opposite effect. We find far stronger enrichment of insertions, especially inter-

chromosomal SDs, near the euchromatin boundaries of chimpanzee, bonobo, and gorilla genomes compared with Asian great apes without subterminal satellites (Fig. 6). More importantly, this enrichment has led to the emergence of 204 species-specific genes (Yoo et al. 2025; Supplemental Tables S6, S7) recently identified in chimpanzee, bonobo, and gorilla. These contain distinct splice junctions and transcript models with open reading frames and thus are candidates for the emergence of novel functional proteins in each species. Therefore, subterminal heterochromatic chromatin (similar to the pericentromeric and SDs at the boundaries of inversions [Linardopoulou et al. 2005; Porubsky et al. 2020; Yoo et al. 2025]) may function as an incubator for the birth of new genes in ape genomes. This implicit genomic instability may confer a long-term selective advantage if the genes evolve function important for the survival of the species.

Methods

Identification of subterminal satellites and SDs

Subterminal satellites or pCht repeats of African great ape genomes, identified by a previous study were used (Yoo et al. 2025). Briefly, African great ape genomes (chimpanzee, bonobo, and gorilla) were screened for pCht satellites via BLASTN (v2.12.0) (Chen et al. 2015) with the consensus sequence (len = 32 bp): "gatatttccatgtttatagatagcgggtga." BLAST hits with >90% of the consensus (>28 bp) were recovered. The individual pCht unit was classified into different types based on the variants (small INS, DEL, or substitution). The SD spacers interrupting the satellite arrays were identified using BEDTools "subtract" option, subtracting the subterminal satellite arrays from the entire subterminal satellite regions, and 32 kbp of highly conserved sequence was identified in the *Pan* lineage and 34 kbp independently in gorilla. For extracting more precise locations of the individual SD spacers, minimap2 (v2.26) (Li 2018) was used ("-x asm20").

The relationship between the subterminal arms shown in Figure 2A was predicted by performing hierarchical clustering implemented by pvclust v2.2 (Suzuki and Shimodaira 2006) analysis, limiting to the most abundant pCht ($n > 100$) (method.dist = "correlation," and method.hclust = "average," nboot = 100). The input matrix fed into pvclust was built by computing normalized counts of 19,012 pChts (count of one pCht variant in a subterminal arm/count of total pCht variants in that subterminal arm) across each subterminal arm. The higher-order structure of subterminal satellites was further investigated based on two-step *k*-means clustering (Hartigan and Wong 1979). The initial *k*-means clustering was performed under the assumption that some combinations of pCht variants are more frequently found together than others. This was done by computing the fraction of each pCht variant ($n = 19,012$) across each of the subterminal arms (Chr1p, Chr1q, etc.). The optimal number of clusters was inferred by selecting the optimal Silhouettes score (Rousseeuw 1987), varying *k* from at least five to 20 groups. The second *k*-means clustering was performed using the cluster of pChts ($n = 6$) across subterminal caps divided into 20 kbp nonoverlapping blocks. Again, the optimal number was determined by computing the Silhouettes score for *k* ranging from five to 20. The second clustering identified a total of eight higher-order blocks of subterminal satellites that contain similar composition of pChts.

Phylogeny of SD spacers

Based on the mutations accumulated in the 32 and 34 kbp SD spacers, phylogeny was inferred using the maximum likelihood approach implemented by IQtree2 (v2.3.6) (Minh et al. 2020). All

SD spacers >90% of original lengths were used. To estimate the position of the root, we identified ortholog copies of the 32 and 34 kbp spacers in the remaining great ape lineages, using siamang as the outgroup (Yoo et al. 2025); the ortholog copies were obtained with minimap2 (Li 2018) (v2.26). The MSA of the SD spacers was generated using MAFFT (v7) (Katoh and Standley 2013). Based on the MSA, two phylogenetic trees of SD spacers were constructed with -B 1000 and with the GTR+F+I+R6 and TVM+F+I+R8 models, which were chosen as the best fit model via Bayesian information criterion, for the gorilla and *Pan* spacer trees, respectively. The trees were timescaled with the syntenic original copies corresponding to the single-copy ortholog of orangutan and siamang. The previously reported divergences between human and chimpanzee, gorilla, orangutan, and siamang of 6.4, 8.6, 15.2, and 19.5 MYA, respectively, were used for the time recalibration (Kumar et al. 2022). We used 100 replicates to compute confidence intervals using IQtree2 parameters, “--date-ci 100.” To check for consistency of the maximum likelihood tree, we additionally constructed a neighbor-joining tree and a maximum parsimony tree using MEGA12 (Kumar et al. 2024).

Analysis of ectopic recombination

Under the assumption that ectopic sequence exchange takes place at subterminal arms, we investigated for evidence of such events via two different approaches, through pairwise comparisons of subterminal arms restricted (1) to SD spacers and (2) to the full sequence. The alignment was performed independently in each species using minimap2 (v2.26) (Li 2018), and the average identity, as well as breadth of coverage, was computed. To locate the representative event, we narrowed down the search space, restricting to the alignment of identity to >99.5% to obtain relatively recent events and to the scale of sequences >1 Mbp.

To investigate locational bias of ectopic sequence exchange breakpoints, we tested their relative distance to the nearest SD spacers. This was done through a simulation test, shuffling the breakpoints 1000 times to generate the null distribution of average distances; the *P*-value was computed by quantifying the fraction of more extreme null values to the observed averages.

We further tested whether the breakpoints of ectopic sequence exchanges fall within SD spacers by computing phylogenetic trees. We divided the MSA of SD spacers into two equally sized regions and constructed the phylogenetic trees of the first and second half of sequences, which were then compared with the original tree computed by the full SD sequences. If the ectopic exchanges take place frequently at the SD spacers, the inferred phylogeny based on the first or second half of the sequence would shift dramatically. To test significance, we generated null distribution by computing the Robinson–Foulds distance between bootstrap trees to that of the consensus trees. This was then compared with the tree built by half of the SD sequences.

Quantification of structural variations at the euchromatic boundaries

The subterminal euchromatic boundaries were defined as the 2 Mbp regions downstream from or upstream of subterminal satellite arrays of p-arms or q-arms, respectively. In the case of species with no subterminal satellites, the boundaries were defined as the 2 Mbp tips. The structural variation calls from PAV (v2.3.2) (Ebert et al. 2021), taking human (T2T-CHM13 v2.0) as the reference and SDs identified from the previous study (Yoo et al. 2025), were used. For the large insertions, we separately inferred the additional sequences of apes relative to humans by using syntenic alignment. The alignment between homologous chromo-

somes between human and nonhuman apes (i.e., Chr1 vs. hsa1) generated by minimap2 (v2.26) was broken using RustyBam (v0.1.29) with a minimum structural event size of 50 bp. The unaligned regions of apes that are missing corresponding human homologs were considered as insertions. We also performed alignment of individual chromosomes to the whole orangutan genome to investigate origins of the inserted sequences.

Methylation

Methylation status of the subterminal cap sequences was determined based on ONT long-read sequencing data as described in a previous study (Yoo et al. 2025; <https://github.com/marbl/T2T-Browser/tree/main/src/epi>). Briefly, the CpG methylation calls were generated from Guppy v6.3.7 using the model “dna_r9.4.1_450bps_modbases_5hmc_5mc_cg_sup_prom.cfg.” Reads were aligned to the genome with minimap2 v2.26, and counts of modified bases at each cytosine position were obtained using modbam2bed v0.10.0. Because CpG methylation is symmetrical, counts from both cytosines in a CpG dinucleotide were merged to represent a single CpG site. Fractional methylation levels were then calculated for CpG sites supported by at least five reads.

Analysis of transcriptome and novel genes

Gene annotations and transcriptome alignment analyzed by the previous study were used (Yoo et al. 2025). Briefly, the transcriptome data were aligned onto respective genome assemblies using minimap2 (v2.26) after generating index via “*minimap2 -ax splice -f 1000 --secondary=no --eqx -K 100M*” and aligning using “*minimap2 -ax splice -f 1000 --secondary=no --eqx*.” StringTie (v3) was used for assessment and quantification of the transcripts (Pertea et al. 2015). Gene Ontology (GO) terms, including biological process, molecular function, and cellular component, of the novel genes located at the subterminal cap boundaries were analyzed using Panther database released on 2024/02/26 (Mi et al. 2019).

Competing interest statement

E.E.E. is a scientific advisory board (SAB) member of Variant Bio. All other authors declare no competing interests.

Acknowledgments

We thank Tonia Brown, Soojin V. Yi, and Dongmin R. Son for helpful comments in the preparation of this manuscript. This work was supported, in part, by funding from the National Institutes of Health (NIH grants R01HG002385 and R01HG010169) and Weill Neurohub Family Foundation support to E.E.E. E.E.E. is an investigator of the Howard Hughes Medical Institute. This article is subject to HHMI’s Open Access to Publications policy. HHMI laboratory heads have previously granted a nonexclusive CC BY 4.0 license to the public and a sublicensable license to HHMI in their research articles. Pursuant to those licenses, the author-accepted manuscript of this article can be made freely available under a CC BY 4.0 license immediately upon publication.

Author contributions: D.Y. performed evolutionary and methylation analyses. D.Y. and E.E.E. wrote the manuscript. K.M.M. provided sequencing support. E.E.E. and K.M.M. reviewed the manuscript. E.E.E. supervised and funded the project.

References

- Chen Y, Ye W, Zhang Y, Xu Y. 2015. High speed BLASTN: an accelerated MegaBLAST search tool. *Nucleic Acids Res* **43**: 7762–7768. doi:10.1093/nar/gkv784
- Ebert P, Audano PA, Zhu Q, Rodriguez-Martin B, Porubsky D, Bonder MJ, Sulovari A, Ebler J, Zhou W, Serra Mari R, et al. 2021. Haplotype-resolved diverse human genomes and integrated analysis of structural variation. *Science* **372**: eabf7117. doi:10.1126/science.abf7117
- Fontserè C, Kuhlwil M, Morcillo-Suarez C, Alvarez-Estape M, Lester JD, Gratton P, Schmidt JM, Dieguez P, Aebischer T, Álvarez-Varona P, et al. 2022. Population dynamics and genetic connectivity in recent chimpanzee history. *Cell Genomics* **2**: 100133. doi:10.1016/j.xgen.2022.100133
- Haaf T, Schmid M. 1987. Chromosome heteromorphisms in the gorilla karyotype: analyses with distamycin A/DAPI, quinacrine and 5-azacytidine. *J Heredity* **78**: 287–292. doi:10.1093/oxfordjournals.jhered.a110389
- Hartigan JA, Wong MA. 1979. Algorithm AS 136: a K-means clustering algorithm. *J R Stat Soc Ser C (Appl Stat)* **28**: 100–108. doi:10.2307/2346830
- Hirai H, Hirai Y, Udono T, Matsubayashi K, Tosi AJ, Koga A. 2019. Structural variations of subterminal satellite blocks and their source mechanisms as inferred from the meiotic configurations of chimpanzee chromosome termini. *Chromosome Res* **27**: 321–332. doi:10.1007/s10577-019-09615-z
- Ijdo JW, Baldini A, Ward D, Reeders S, Wells R. 1991. Origin of human chromosome 2: an ancestral telomere-telomere fusion. *Proc Natl Acad Sci* **88**: 9051–9055. doi:10.1073/pnas.88.20.9051
- Jiang X, Zhang L, Yang Z, Yang X, Ma K, Yoo D, Lu Y, Zhang S, Chen J, Nie Y, et al. 2024. Incomplete lineage sorting of segmental duplications defines the human chromosome 2 fusion site early during African great ape speciation. *bioRxiv* doi:10.1101/2024.12.12.628057
- Katoh K, Standley DM. 2013. MAFFT multiple sequence alignment software version 7: improvements in performance and usability. *Mol Biol Evol* **30**: 772–780. doi:10.1093/molbev/mst010
- Knight SJ, Flint J. 2000. Perfect endings: a review of subtelomeric probes and their use in clinical diagnosis. *J Med Genet* **37**: 401–409. doi:10.1136/jmg.37.6.401
- Koga A, Notohara M, Hirai H. 2011. Evolution of subterminal satellite (StSat) repeats in hominids. *Genetica* **139**: 167–175. doi:10.1007/s10709-010-9534-0
- Koga A, Hirai Y, Hara T, Hirai H. 2012. Repetitive sequences originating from the centromere constitute large-scale heterochromatin in the telomere region in the siamang, a small ape. *Heredity (Edinb)* **109**: 180–187. doi:10.1038/hdy.2012.28
- Kumar S, Suleski M, Craig JM, Kasprowicz AE, Sanderford M, Li M, Stecher G, Hedges SB. 2022. TimeTree 5: an expanded resource for species divergence times. *Mol Biol Evol* **39**: msac174. doi:10.1093/molbev/msac174
- Kumar S, Stecher G, Suleski M, Sanderford M, Sharma S, Tamura K. 2024. MEGA12: molecular evolutionary genetic analysis version 12 for adaptive and green computing. *Mol Biol Evol* **41**: msae263. doi:10.1093/molbev/msae263
- Li H. 2018. Minimap2: pairwise alignment for nucleotide sequences. *Bioinformatics* **34**: 3094–3100. doi:10.1093/bioinformatics/bty191
- Linardopoulou EV, Williams EM, Fan Y, Friedman C, Young JM, Trask BJ. 2005. Human subtelomeres are hot spots of interchromosomal recombination and segmental duplication. *Nature* **437**: 94–100. doi:10.1038/nature04029
- Liu Y, Liu Z, Jiang T, Zang T, Wang Y. 2022. Comparison of the nanopore and PacBio sequencing technologies for DNA 5-methylcytosine detection. *IEEE International Conference on Bioinformatics and Biomedicine (BIBM)*, Las Vegas, NV, pp. 220–225. IEEE, Piscataway, NJ. doi:10.1109/BIBM55620.2022.9995567
- Makova KD, Pickett BD, Harris RS, Hartley GA, Cechova M, Pal K, Nurk S, Yoo D, Li Q, Hebbar P, et al. 2024. The complete sequence and comparative analysis of ape sex chromosomes. *Nature* **630**: 401–411. doi:10.1038/s41586-024-07473-2
- Mao Y, Harvey WT, Porubsky D, Munson KM, Hoekzema K, Lewis AP, Audano PA, Rozanski A, Yang X, Zhang S, et al. 2024. Structurally divergent and recurrently mutated regions of primate genomes. *Cell* **187**: 1547–1562.e13. doi:10.1016/j.cell.2024.01.052
- McConkey E. 2004. Orthologous numbering of great ape and human chromosomes is essential for comparative genomics. *Cytogenet Genome Res* **105**: 157–158. doi:10.1159/000078022
- Mefford HC, Trask BJ. 2002. The complex structure and dynamic evolution of human subtelomeres. *Nat Rev Genet* **3**: 91–102. doi:10.1038/nrg727
- Mi H, Muruganujan A, Huang X, Ebert D, Mills C, Guo X, Thomas PD. 2019. Protocol update for large-scale genome and gene function analysis with the PANTHER classification system (v. 14.0). *Nat Protoc* **14**: 703–721. doi:10.1038/s41596-019-0128-8
- Minh BQ, Schmidt HA, Chernomor O, Schrempf D, Woodhams MD, von Haeseler A, Lanfear R. 2020. IQ-TREE 2: new models and efficient methods for phylogenetic inference in the genomic era. *Mol Biol Evol* **37**: 1530–1534. doi:10.1093/molbev/msaa015
- Novo C, Arnoult N, Bordes WY, Castro-Vega L, Gibaud A, Dutrillaux B, Bacchetti S, Londoño-Vallejo A. 2013. The heterochromatic chromosome caps in great apes impact telomere metabolism. *Nucleic Acids Res* **41**: 4792–4801. doi:10.1093/nar/gkt169
- Nurk S, Koren S, Rhie A, Rautiainen M, Bizikadze AV, Mikheenko A, Vollger MR, Altemose N, Uralsky L, Gershman A, et al. 2022. The complete sequence of a human genome. *Science* **376**: 44–53. doi:10.1126/science.abj6987
- Pertea M, Pertea GM, Antonescu CM, Chang TC, Mendell JT, Salzberg SL. 2015. StringTie enables improved reconstruction of a transcriptome from RNA-seq reads. *Nat Biotechnol* **33**: 290–295. doi:10.1038/nbt.3122
- Porubsky D, Sanders AD, Höps W, Hsieh P, Sulovari A, Li R, Mercuri L, Sorensen M, Murali SC, Gordon D, et al. 2020. Recurrent inversion toggling and great ape genome evolution. *Nat Genet* **52**: 849–858. doi:10.1038/s41588-020-0646-x
- Porubsky D, Guitart X, Yoo D, Dishuck PC, Harvey WT, Eichler EE. 2024. SVbyEye: a visual tool to characterize structural variation among whole-genome assemblies. *Bioinformatics* **41**: btaf332. doi:10.1093/bioinformatics/btaf332
- Rousseeuw PJ. 1987. Silhouettes: a graphical aid to the interpretation and validation of cluster analysis. *J Comput Appl Math* **20**: 53–65. doi:10.1016/0377-0427(87)90125-7
- Royle NJ, Baird DM, Jeffreys AJ. 1994. A subterminal satellite located adjacent to telomeres in chimpanzees is absent from the human genome. *Nat Genet* **6**: 52–56. doi:10.1038/ng0194-52
- Sigurpalsdottir BD, Stefansson OA, Holley G, Beyter D, Zink F, Hardarson MP, Sverrisson SP, Kristinsdottir N, Magnúsdóttir DN, Magnússon OP, et al. 2024. A comparison of methods for detecting DNA methylation from long-read sequencing of human genomes. *Genome Biol* **25**: 69. doi:10.1186/s13059-024-03207-9
- Suzuki R, Shimodaira H. 2006. Pvcust: an R package for assessing the uncertainty in hierarchical clustering. *Bioinformatics* **22**: 1540–1542. doi:10.1093/bioinformatics/btl117
- Ventura M, Catacchio CR, Alkan C, Marques-Bonet T, Sajjadian S, Graves TA, Hormozdiari F, Navarro A, Malig M, Baker C, et al. 2011. Gorilla genome structural variation reveals evolutionary parallelisms with chimpanzee. *Genome Res* **21**: 1640–1649. doi:10.1101/gr.124461.111
- Ventura M, Catacchio CR, Sajjadian S, Vives L, Sudmant PH, Marques-Bonet T, Graves TA, Wilson RK, Eichler EE. 2012. The evolution of African great ape subtelomeric heterochromatin and the fusion of human chromosome 2. *Genome Res* **22**: 1036–1049. doi:10.1101/gr.136556.111
- Vollger MR, Kerpedjiev P, Phillippy AM, Eichler EE. 2022. StainedGlass: interactive visualization of massive tandem repeat structures with identity heatmaps. *Bioinformatics* **38**: 2049–2051. doi:10.1093/bioinformatics/btac018
- Yoo D, Rhie A, Hebbar P, Antonacci F, Logsdon GA, Solar SJ, Antipov D, Pickett BD, Safonova Y, Montinaro F, et al. 2025. Complete sequencing of ape genomes. *Nature* **641**: 401–418. doi:10.1038/s41586-025-08816-3
- Yunis JJ, Prakash O. 1982. The origin of man: a chromosomal pictorial legacy. *Science* **215**: 1525–1530. doi:10.1126/science.7063861

Received May 29, 2025; accepted in revised form October 11, 2025.